

# RESEARCH MEMORANDUM

PRELIMINARY INVESTIGATION OF SEVERAL ROOT DESIGNS FOR  
CERMET TURBINE BLADES IN TURBOJET ENGINE

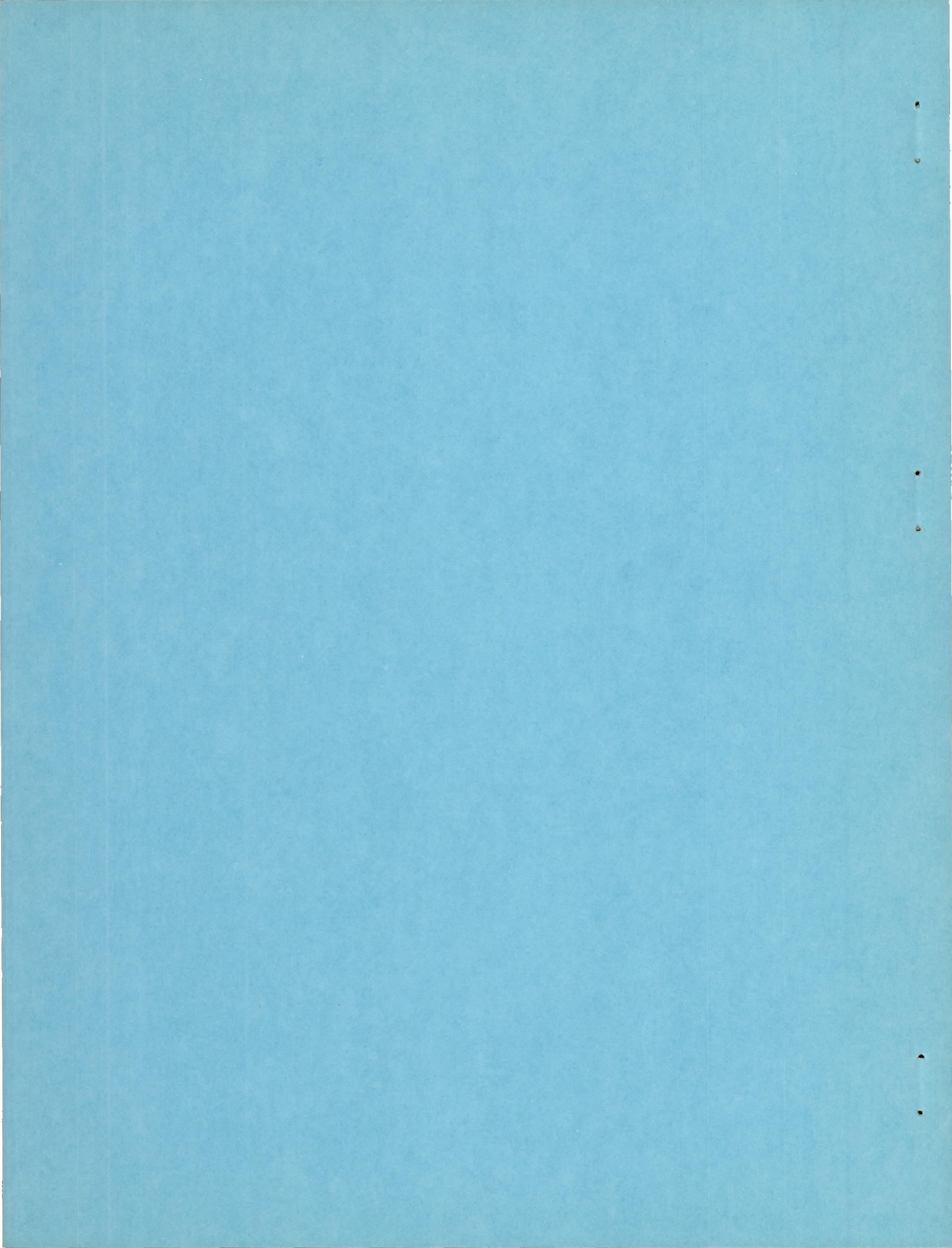
II - ROOT DESIGN ALTERATIONS

By A. J. Meyer, Jr., G. C. Deutsch, and W. C. Morgan

Lewis Flight Propulsion Laboratory  
Cleveland, Ohio

NATIONAL ADVISORY COMMITTEE  
FOR AERONAUTICS

WASHINGTON  
October 13, 1953



NATIONAL ADVISORY COMMITTEE FOR AERONAUTICS

RESEARCH MEMORANDUM

PRELIMINARY INVESTIGATION OF SEVERAL ROOT DESIGNS FOR CERMET

TURBINE BLADES IN TURBOJET ENGINE

II - ROOT DESIGN ALTERATIONS

By A. J. Meyer, Jr., G. C. Deutsch, and W. C. Morgan

SUMMARY

Twelve engine evaluation tests of cermet turbine blades are reported herein. The first five runs were similar to the ten engine tests reported previously. The cermet blades were then redesigned on the basis of information gained during the earlier runs. The profile of the root was changed; the airfoil was relocated on the platform and root; the root center line was rotated with respect to the turbine axis; and an attempt was made to improve the blade material. These alterations primarily accomplished a reduction in root bending stresses and resulted in greatly increased blade life.

The modified blades were operated under increased power output from the engine and were subjected to cyclic conditions between take-off speed and idling speed.

INTRODUCTION

The information reported herein is a continuation of an investigation at the NACA Lewis laboratory to devise methods of utilizing ceramic-metal materials as turbine blades for use in aviation jet-propulsion engines. The first full-scale engine runs with cermet blades are described in reference 1. Principally in order to evaluate blade root design, blades made from the same material and supplied by the same manufacturer were again tested. The blade root was completely redesigned to reduce the excessive bending stresses which were indicated by the characteristics of the fracture surfaces obtained in the first ten runs described in reference 1 and five additional runs included in this report. The new blades were subjected to the same type of operation used in previous engine tests and, in addition, to operation at full take-off power (early tests were conducted at reduced power to increase the life of engine parts other than blades) and a limited amount of cyclic operation.

## DESCRIPTION OF CERMET BLADES

The blade airfoils were the same shape and size as the airfoils for the standard metal blades. The root designs for the interlock and dovetail blades (runs 11-13 and 17) were the same as used in previous engine runs, numbers 5 to 7, 9, and 10 of reference 1, in which four root designs and four materials were partly evaluated by operation in a full-scale engine. All cermet roots were developed in accordance with procedure outlined in reference 2 which describes the results of rupture tests of plastic models of 18 different root designs and establishes the criteria for the design of brittle material blade roots. The skewed dovetail root profile (runs 14-16) was designed to meet the optimum proportions as established in the same reference.

The composition for all the blades used in engine runs 11, 11A, and 13 through 17 and for two of the blades of run 12A was titanium carbide containing 30 percent nickel by weight and with 8 percent of a solid solution of the carbides of columbium, tantalum, and titanium added to improve oxidation resistance. The blades of run 12 were of composite construction: the airfoils were of the composition noted previously, while the roots contained 50 percent instead of 30 percent nickel by weight. The additional nickel was provided to increase the ductility in the root or the region where high-temperature properties could be sacrificed to obtain added toughness. The added nickel decreased the hardness to the point where the root could be filed and thus diamond wheels should not be required for final root finishing. The transition zone between the 30 and 50 percent nickel regions was approximately 0.050 inch wide and occurred at the top of the platform.

All cermet blades were produced by Kennametal Inc. The blades were inspected with penetrant oil and radiographic methods prior to engine operation.

## ENGINE TESTS PRIOR TO BLADE REDESIGN

A summary of the pertinent data for the engine runs is shown in table I. The run numbers are continued in chronological order following the 10 previous engine tests reported in reference 1. Those runs in which a majority of the blades were used in the preceding run are designated with the suffix "A" added to the original number.

Interlock blade runs, run 11. - Run 11 utilized blades similar to those of run 10 (ref. 1), which lasted for 68 hours at rated speed, except that the airfoil was of normal thickness instead of increased 0.040 inch as was the case in run 10. Run 11 should have operated longer than run 10 because the root stresses at which the blade failed were 20 percent less as a result of the use of normal airfoil thickness.

One root, however, failed after only 6 minutes at rated speed (11,750 rpm) and the fractured surface is shown in figure 1. Figure 2 shows the location of the failed blade with respect to the other cermet and the metal blades.

Run 11A. - Because the apparent damage to the other cermet blades in run 11 was very slight, and after penetrant-oil inspection indicated that these blades were still sound, the failed blade was replaced and the wheel was rebalanced. This assembly did not attain rated speed but failure occurred in the airfoil during acceleration at 50 rpm below rated speed. Possibly the failure resulted from a defect in the previously used blades which was not detected during inspection. The broken cermet airfoils are shown in figure 3.

Run 12. - Run 12 was also conducted with six cermet interlock blades; however, the metal content in the root was increased from 30 percent to 50 percent by weight. The objective of the change was to increase the ductility and thus reduce the notch sensitivity and thereby provide increased life in the engine. The change however did not prove beneficial because a root failure occurred after 7 minutes at rated speed. The failure is shown in figure 4. Again the damage to the other cermet blades was very slight and therefore only two of the blades were replaced with cermet blades of uniform composition.

At this point in the program it became apparent that in all the runs using six cermet blades and involving root failures (runs 8 to 12) the failure was always adjacent to a metal blade (figs. 2 and 4). The center cermet blade in a group of three failed only in run 10 and, in this case, all three cermet blades on one side of the turbine wheel failed in the root making it impossible to determine where the failure originated. Looking from the rear of the turbine, the root failures occurred mostly in the blade which was farthest in the clockwise direction (opposite to the direction of rotation); the only exception was run 8 with the pin-type root design where the blade farthest in the counterclockwise direction failed first. The metal blades were 50 percent heavier than the cermet blades because of the differences in material densities. This factor undoubtedly imposed an unsymmetrical loading condition on the turbine wheel segment between the metal and the cermet blade and is considered to have had an effect on which blade failed first. Why the clockwise-most blade generally failed was not known.

Run 12A. - In order to offset the effect of the heavier-metal blade, half the airfoil in run 12A was cut off the two diametrically opposite metal blades adjacent to the clockwise-most cermet blade in each group of three blades. The results of engine testing the assembly are shown in figure 5. Two adjacent cermet blades failed in the roots after 5 minutes at rated speeds. It is impossible to establish which of the two roots failed first. The difference in grain structure apparent in the figure is caused by different compositions; the lower root in the photograph was made with 50 percent nickel binder while the other was 30 percent nickel.

Dovetail blade, run 13. - It was not understood why it appeared impossible to exceed or at least duplicate the 58- and 68-hour runs for the dovetail (run 9) and interlock (run 10), respectively, reported in reference 1. The root designs and the material composition of the later blades were supposedly identical to those of the blades used in the earlier runs. The quality of the material and of the machining was suspected. In an attempt to isolate the poor blades from the good ones, a set of 12 blades was cold-spun to 20 percent overspeed and consequently to 44 percent over the normal operating stress. The six surviving blades (the other six failed in the range between 10 and 20 percent overspeed) were installed in the turbine rotor along with two shortened metal blades. This group of blades (run 15) failed after 16 minutes at 11,750 rpm. Two roots failed, both adjacent to metal blades and both on the same side of the rotor as shown in figure 6. The intervening cermet blade failed in the airfoil. As can be seen in the photograph, the turbine was instrumented with thermocouples to measure temperatures in the vicinity of the cermet root. However, the unit did not operate long enough at rated speed for the rotor temperatures to become stabilized. Figure 7 shows the fracture surfaces of the two root failures and shows small parts of the screen used between rotor and blade. The spalled appearance of the fractures indicates that the compressive stresses due to either bearing loads or thermal expansion, or both, were too high as contrasted with the clean tensile failures of figures 1, 4, and 5.

#### REDESIGN OF CERMET BLADE

As mentioned earlier, the root failures occurred consistently adjacent to the metal blades. Examination of interlock root failures showed that all the fractures seemed to originate in exactly the same area, near the center of the root length and on the side of the root cross section corresponding to the suction or convex side of the airfoil (figs. 1, 4, and 5). These facts suggested that load distribution in the root was unfavorable and that the blade should be redesigned to improve this condition. Up to this point all airfoils were located on the platforms in precisely the same manner as were the metal blades in the standard engine, and the root center lines were parallel to the turbine axis.

#### Location of Center of Gravity of the Airfoil

If the profile of the airfoil at its base is superimposed on the photograph of a fractured root surface (fig. 8), it becomes apparent that the failure invariably starts at the location of the largest concentration of mass of the airfoil. The presence of bending stresses in the root neck is evident because the failure generally starts at the

same side of the root cross section. To verify this conclusion, it was necessary to determine the center of gravity of the whole airfoil. There are several means of determining center of gravity location. Two different methods were used for this report. One was the method fully described in reference 3. The other method, which is described in the following paragraphs, is very useful because it not only locates the center of gravity but also provides an approximate indication of the tensile stress distribution at the base plane of the airfoil and also the bending moment distribution acting on the root cross section. The locations of the center of gravity of the whole airfoil as determined by the two methods were in close agreement.

Calculation procedure. - The airfoil span or length was divided into 10 sections. The profiles of the sections were drawn to five times the size. The base profile was subdivided into small squares 1/2 inch on a side (0.1 inch on a side at actual blade size.) All other profiles were correspondingly subdivided into rectangles 1/2 inch in the direction of the turbine wheel axis and slightly greater than 1/2 inch in the tangential direction. The correction in tangential distance is due to the increase in chord length of a radial segment as the radial distance increases, as sketched diagrammatically in figure 9. The volumes of the small airfoil pieces between corresponding rectangles of each station were calculated and totalled. The centers of gravities and the radial distances of the resulting long thin radial columns were computed to permit calculation of the centrifugal force acting on each square of the base airfoil profile due to its respective column.

Results of calculation. - The results of the calculations are shown in figure 10. The upper numbers in each square are the total centrifugal forces in pounds acting on each square and the lower numbers (under-scored) are the stresses (in 1000-psi units) that would be acting on the base plane squares if each column were cut free from its neighbors. Actually, there would be a gradual variation in stress from one square to the next. From the magnitude of the numbers presented and their location, it is obvious that the greatest centrifugal loads and stresses are in the region where most of the failures originated. The location of the radial projection of the center of gravity of the whole airfoil is determined by dividing the summation of moments of the centrifugal force of the individual columns times their distance from an arbitrary axis by the summation of the centrifugal forces.

Effect of offset center of gravity. - The procedure described shows the projection of the center of gravity on the base plane to be displaced 0.051 inch in the direction of rotation from the center line of the blade platform and root. This offset introduces a sizable bending moment in the blade root which is only partly compensated for by the gas forces on the airfoil. The gas force per blade as determined in the appendix of this report is 100 pounds at rated speed and

power. Assuming this force is concentrated at the center of pressure of the airfoil, the gas force moment about the root neck is 247 inch-pounds. The total centrifugal force of the airfoil alone is 11,300 pounds and its moment due to the 0.051-inch offset is 575 inch-pounds. The net bending stress  $S$  caused by the net moment is approximated by:

$$S = \frac{Mc}{I}$$

where

$M$  bending moment (575 - 247 = 328 in.-lb)

$c$  distance from neutral axis to outermost fiber, 0.190 inch for interlock root

$I$  moment of inertia =  $\frac{bh^3}{12}$

$b$  root length, 1.96 inches for all roots tested in this report

$h$  root width, 0.379 inch for interlock root design

The bending stress resulting from this computation is  $\pm 6990$  pounds per square inch. If then the airfoil is shifted 328 divided by 11,300, or 0.029 inch, in the tangential direction toward the concave or pressure side of the blade, this bending stress can be virtually eliminated.

#### Skewing the Blade Root

Further improvements of the stress distribution in the blade roots can be made by skewing or rotating the blade root center line with respect to the airfoil and turbine axis. Effectively this means reducing the amount of overhang of the trailing edge and of the suction side towards the leading edge of the airfoil with respect to the cross-sectional area of support at the root neck.

Determination of skewing angle. - The skewing angle was established by finding the centers of gravity of the leading and trailing halves of the airfoil. Assume that the blade is cut lengthwise by a dividing plane through the midchord points and perpendicular to the turbine axis. Then the radial projection of the centers of gravity of each half on the base plane can be readily calculated from the previous computations, and a line drawn through these centers was used to determine the skewing angle, which in this case is  $14.4^\circ$  (see fig. 11).



The root center line should be offset from the line thus established sufficiently (0.022 inch in this case) to compensate for the bending moment caused by the gas force. In figure 11, the numbers within the airfoil are the products of the centrifugal force of the long thin individual columns used earlier and their distance from the old (parallel to turbine axis) and new (skewed) center lines of the platform and root. The lower numbers (underlined) in each square are for the old center line and the upper numbers correspond to the skewed center line. The exact values of these numbers are not a direct measure of the actual stress distribution in the root, but the relative magnitudes of the numbers are indicative of the amount of overhang or the stress magnitude in corresponding areas in the root.

Effect of skewed root. - The largest number with the old center line is 1110, square 2-H, which might intimate that failure should have started in the root below the trailing edge. However, surrounding values are considerably less and thus would tend to reduce the peak stress at this location. The second largest number with the old center line is 1007, square 13-B, and is flanked by similar high values and therefore would be expected to influence the point where the root failures originated. The actual failure did start in this area.

The largest number with respect to the new center line is 658 (square 11-B), or appreciably less than the largest with the old axis. The 1110 value is reduced to 551, or by about one half. The 1007 value is also about halved, or is 582. The values in the vicinity of the leading edge are multiplied four or five times, but the values are still relatively low because the leading edge of the airfoil is swept back rapidly as the distance from the turbine axis increases. Consequently, skewing the blade root with respect to the airfoil and turbine axis should prove very beneficial.

#### Root Profile

The results of a separate investigation on root profile design are reported in reference 2. In this reference optimum root proportions were determined to give maximum strength in pure tension. The experimental failure load for the small-radius dovetail profile is 37,190 pounds. When the optimum proportions of reference 2 are used, the same load is 41,220 pounds, or an improvement of 11 percent, as established by tensile tests of cermet specimens at 1200° F, reference 4. The increase was caused by a decreased stress concentration factor resulting from increasing the notch radius in the root from 0.156 inch to 0.280 inch. The neck distance in the root had to be reduced from 0.438 inch to 0.405 inch to accommodate the larger-radius root; nevertheless, it is stronger as a result of the lower stress concentration factor. The new root including both the skewing and the new profile is sketched along with the earlier dovetail for comparison in figure 12.

## ENGINE OPERATION FOLLOWING REDESIGN

The blade manufacturer concurrently has been investigating the processing and methods of machining blade roots and has reported a considerable improvement on the blade material. New blades with improved fabrication techniques and incorporating the latest changes were assembled in the turbojet engine. Four cermet blades were used because it was impossible to install the same number of skewed roots in the space originally provided for six blades in the conventional turbine rotor. The blades were placed in diametrical pairs with normal spacing between the two cermet blades comprising each pair. The spacing between the cermet and the metal blade consequently was greatly increased, thus reducing the effect of the unsymmetrical loading in the rotor segments due to the heavier metal blades.

Run 14. - The engine with the new blades ran 112.5 hours before disassembly for over-all inspection. Run 14 and all previous runs with cermets were run with slightly opened tail cone because other engine parts cannot withstand continuous operation at rated power and speed, 11,750 rpm. Rotational speed and not power is the most important criterion determining the life of cermet blades. However, to include any additional effects that may be precluded by the limited power operation, the same four cermet blades were next operated at full power for 17 hours, at which time the nozzle diaphragm shroud failed and broke the cermet airfoils (fig. 13), completing run 14 of table I. Figure 14 shows the missing piece of the shroud band which passed through the turbine. The tail cone assembly had to be replaced frequently during the full-power operation and also the combustion-chamber tube assembly was excessively cracked.

Run 15. - For run 15, the engine was completely rebuilt and four more of the redesigned blades were tested. These blades were subjected to 50 hours at maximum power and speed without mishap. To evaluate the thermal shock properties of the root design and the blade material, the engine was cycled. Cyclic operation consists in running 15 minutes at rated power and speed (11,750 rpm) followed by 5 minutes at idling conditions (4000 rpm), with rapid acceleration and deceleration between these conditions. The cycle was successfully completed 13 times but after 1 minute at full power in the 14th cycle, two of the cermet blades on the same side of the wheel failed in the root, terminating run 15 (fig. 15). It can be noticed in the photograph that one of the fractures is a clean break without evidence of bending stresses. The second slightly rougher break is probably the result of impact from the first blade. The broken tip section of the airfoil of the metal blade shown in figure 15, incidentally, is the first metal blade failure caused by impact from cermet blades.

Run 16. - Runs 14 and 15 indicated that an improvement had been accomplished in the redesigned blades but several changes had been incorporated at one time. The root was displaced slightly with respect to the airfoil and was skewed, the notch radius was increased, and attempts had been made to improve the material. To evaluate which changes were primarily responsible for the increased life, six blades of the unskewed interlock design were fabricated from the same material and by the same processes as the cermet blades of runs 14 and 15. These interlock blades were tested in the engine with slightly opened tail cone in the same manner as all earlier tests and the first part of run 14. As noted in the table, these blades lasted only 58 minutes at rated speed, indicating that any material changes were not the major cause for increased life. As shown in figure 16, the failure occurred for the first time between two cermet blades and not adjacent to a metal blade.

To determine whether the increased life was the result of displacing and skewing the root or the increased notch radius, several skewed-root blades of the original dovetail profile with the smaller notch radius were ordered. Furthermore, it was hypothesized that the cyclic failure of run 15 may possibly be the result of having too shallow a wedge angle on the dovetail root with large radius. Tangents to all points of the bearing surface form small, shallow angles with respect to the radial center line of the blade; effectively the root forms a shallow wedge tending to pry open the wheel recess. After a few minutes of high-speed operation, the new blade is very tight in the wheel because of thermal expansion and centrifugal force. At idle condition, the blade root and wheel segments contract thermally but the idling speed, 4000 rpm, is sufficient to throw the blade radially outward taking up all clearance. As the engine attains maximum speed, again the root and wheel segment expand, which must result in plastic flow of the wheel material. This process is repeated with each additional cycle and each time the compressive stresses become a little greater because the materials become less and less susceptible to additional deformation. The bearing surface of the dovetails with small notch radii is more nearly normal or perpendicular to the radial center line of the blade. Therefore, when thermal expansion takes place, the small-radius blade is drawn radially inward instead of being squeezed as the large-radius blades are. Even after 50 hours of rated-speed operation, the old dovetail blades were loose in the turbine recesses when the engine was shut down.

Run 17. - To evaluate the foregoing hypothesis concerning notch radii differences, four skewed-root blades were inserted in a new turbine wheel, two of the large-radius profile on one side of the wheel and two of the small-radius profile on the diametrically opposite side. The intention in run 17 was to run the engine 50 hours at rated speed and power (closed tail cone) and then proceed with cyclic operation. The engine ran 36 hours before the blades were damaged (fig. 17)

as a result of fatigued fragments breaking loose from the combustion domes and liners and passing through the turbine. Even though no cyclic operation was obtained to evaluate the effect of thermal expansion and contraction on the different radii, sufficient operating time was obtained at full power to indicate that probably the displacing and skewing of the root, and not the change in profile, were the primary factors leading to increased blade life.

Run 18. - For run 18, the turbine wheel was rebladed in the same manner as in run 17. The decision was made to run only 10 hours steadily at rated condition before beginning cyclic operation. The blades, however, ran only 6 hours before one of the large-radius blades failed in the root and it broke the second large-radius blade by impact as evidenced by the fracture. The failures are shown in figure 18.

Run 19. - New blades were installed and the run was repeated. As noted in table I under run 19, a small-radius blade failed in the root after only 16 minutes (fig. 20). The cause for this premature failure is unknown.

Run 20. - The conditions of run 18 were repeated for run 20. This time the 10 hours of steady-speed operation were successfully completed and then were followed by cyclic operation. After 103 cycles, a metal blade failed in the airfoil. The failure mechanism was one of stress-to-rupture which originated in a small nick in the leading edge. The cermet blades were not damaged when the metal blade failed; consequently, only a few damaged metal blades were replaced and the testing was continued. Five additional cycles were completed, bringing the total to 108 cycles before one of the cermet blades with the large-radius root failed in the root (fig. 20). The spalled appearance of the fracture indicates that failure was caused by compression from thermal action or excessive bearing stresses and was not caused by the tensile load acting in the root neck. From the test it can be concluded that the material has sufficient thermal shock resistance to be suitable for jet-engine application. The run also confirmed the previous conclusion that skewing the root is mainly responsible for gains in cermet blade life, but the results were inconclusive in evaluating the merits of the large-radius versus the small-radius root.

#### SUMMARY OF RESULTS

The first five engine tests reported herein, runs 11-15, resulted in very short lives at rated-speed conditions. The appearance of the fractured root surfaces indicated the presence of bending stresses in the blade roots. Also, root failures consistently occurred adjacent to the heavier metal blades. To overcome these difficulties, the following five changes were made to future blades:

1. The root was displaced with respect to the airfoil to reduce bending stresses.

2. The root and platform were skewed  $14.4^\circ$  to reduce the overhang at the trailing edge and at midchord position on the convex side of the blade.

3. The optimum root profile proportions were used.

4. The blades were made from refined quality material.

5. Two blades were inserted in the space originally occupied by three blades, thus reducing the bending effect of the heavier metal blades in adjacent slots.

These changes resulted in an increased engine life. A successful run with the previous dovetail profiles (small radius) proved that the profile change was not a major contributing factor to the increased life. A test with the refined material, with all other conditions the same as in the early runs, indicated that the material also was not the prime factor causing the increased life. Consequently it was concluded that offsetting and skewing the blade root was the leading factor responsible for the increased blade life. Successful cyclic operation with these cermet blades indicates that the material has sufficient thermal shock resistance for turbine blades of a jet-propulsion engine.

Lewis Flight Propulsion Laboratory  
National Advisory Committee for Aeronautics  
Cleveland, Ohio, July 6, 1953 .

## APPENDIX - GAS FORCES ACTING ON THE AIRFOIL

In order to estimate the bending taking place in the root, the gas forces on the blade must be established. The horsepower absorbed by the centrifugal compressor of the test engine is given by the following thermodynamic equation:

$$hp = \frac{\gamma R w}{J(\gamma-1)} 42.4 \frac{T_1}{\eta} \left[ \left( \frac{P_2}{P_1} \right)^{\frac{\gamma-1}{\gamma}} - 1 \right]$$

where:

- $\gamma$  ratio of specific heats, 1.4 for air
- $R$  gas constant, 53.3 ft-lb/lb- $^{\circ}$ R for air
- $w$  mass flow, lb/min (5340 lb/min for test engine)
- $J$  mechanical equivalent of heat, 778 ft-lb/Btu
- $T_1$  inlet air temperature, 530 $^{\circ}$  R for this case
- $\eta$  compressor efficiency (assumed 78 percent)
- $P_2/P_1$  compressor pressure ratio (4.6 for subject engine)

The horsepower hp as obtained with this expression is 11,200 horsepower. The gas force now acting on each blade is found from:

$$F = \frac{hp \ 63,030}{nNr}$$

where:

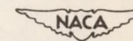
- $n$  number of blades, 54 in this case
- $N$  rotational speed at given horsepower, 11,750 rpm
- $r$  radial distance from axis of rotation at center of pressure on airfoil, 11.125 inches for this unit.

The gas force then is 100 pounds per blade at rated speed and power.

## REFERENCES

1. Deutsch, George C., Meyer, Andre J., Jr., and Morgan, William C.: Preliminary Investigation in J33 Turbojet Engine of Several Root Designs for Ceramal Turbine Blades. NACA RM E52K13, 1953.
2. Meyer, André J., Jr., Kaufman, Albert, and Caywood, William C.: The Design of Brittle-Material Blade Roots Based on Theory and Rupture Tests of Plastic Models. NACA RM E53C12, 1953.
3. Gendler, Sel, and Johnson, Donald F.: Determination of Minimum Moments of Inertia of Arbitrary Shaped Areas, Such as Hollow Turbine Blades. NACA RM E9H10, 1950.
4. Meyer, André J., Jr., Kaufman, Albert, and Calvert, Howard F.: Comparative Tensile Strengths at 1200° F of Various Root Designs for Cermet Turbine Blades. NACA RM E53C25, 1953.

TABLE I. - SUMMARY OF CERMET BLADE ENGINE OPERATION



Run	Root design	Number of cermet blades	Additions to titanium carbide	Test cycle	Total operating time		Time at rated speed		Remarks
					hr	min	hr	min	
11	Interlock	6	30 percent Ni + 8 percent (Cb,Ta,Ti)C	Idle at 4000 rpm. Raised to 9000 rpm in 1000-rpm 3-min-duration steps. Raised to rated speed in 500-rpm 3-min-duration steps	0	39	0	6	One root failure of cermet blade adjacent to metal blade. Failure appeared to originate in root on side corresponding to convex side of airfoil.
11A	Interlock	5 from run 11 + 1 new	30 percent Ni + 8 percent (Cb,Ta,Ti)C	Same as run 11	0	34	0	0	All cermet airfoils failed. (reached 11,700 rpm)
12	Interlock	6	8 percent (Cb,Ta,Ti)C + root 50 percent Ni + airfoil 30 percent Ni	Same as run 11	0	43	0	7	Same as run 11. Remaining cermet blades undamaged.
12A	Interlock	4 from run 13 + 2 new	Same as run 12 Whole blade 30 percent Ni + 8 percent (Cb,Ta,Ti)C	Same as run 11	1	2	0	5	Two adjacent root failures; one 50 percent Ni and other 30 percent Ni. Failures appeared to originate on side corresponding to convex side of airfoil.
13	Dovetail	6	30 percent Ni + 8 percent (Cb,Ta,Ti)C	Same as run 11	1	12	0	16	Two root failures, both adjacent to metal blades. Cold spun prior to engine operation.
14	Skewed dovetail	4	Same as run 11	Same starting cycle as run 11; continuous operation at rated speed for day. Subsequent starts slow acceleration requiring 10 min	117	13	112	32	All cermet blades in good condition. Shut down for complete engine overhaul.
				Total	17	36	16	56	Closed tail cone to obtain maximum thrust. All airfoils damaged by nozzle shroud failure.
				Total	134	49	129	28	
15	Skewed dovetail	4	Same as run 11	Same as run 14 After reaching rated speed, cycled 15 min at rated, 5 min at idle; rapid acceleration and deceleration between rated and idle	52	47	50	00	Operation at maximum thrust. Shut down for overhaul.
				Total	4	33	3	16	Completed 13 cycles. Two adjacent roots failed after 1 min at rated speed in 14th cycle.
				Total	57	20	53	16	
16	Interlock	6	Same as run 11	Same as run 11	1	31	0	58	One root failed between the other cermet blades. Opened tail cone (same as runs 11-13).
17	Skewed dovetail	2 large radius, 2 small radius	Same as run 11	Same as run 11	39	44	36	9	Closed tail cone to produce maximum thrust. Blades failed as a result of failures in combustion domes and liner.
18	Skewed dovetail	2 large radius, 2 small radius	Same as run 11	Same as run 11	6	13	6	1	Closed tail cone. Two large-radius blades failed in root; one was of questionable quality. Small-radius blade undamaged.
19	Skewed dovetail	2 large radius, 2 small radius	Same as run 11	Same as run 11	0	59	0	16	Closed tail cone. One small-radius blade failed in root.
20	Skewed dovetail	2 large radius, 2 small radius	Same as run 11	Same as run 11 Cyclic operation; 15 min at rated power and 5 min at idle with rapid acceleration and deceleration between. Cyclic operation	12	33	11	0	Closed tail cone.
				Total	36	6	25	48	103 cycles completed. Metal blade failed in airfoil. Cermet blades were undamaged.
				Total	48	39	36	48	
				Total	1	39	1	29	5 additional cycles (total of 108 cycles). One large-radius blade failed in root and damaged other large-radius blade at airfoil by impact.
				Total	50	18	38	17	



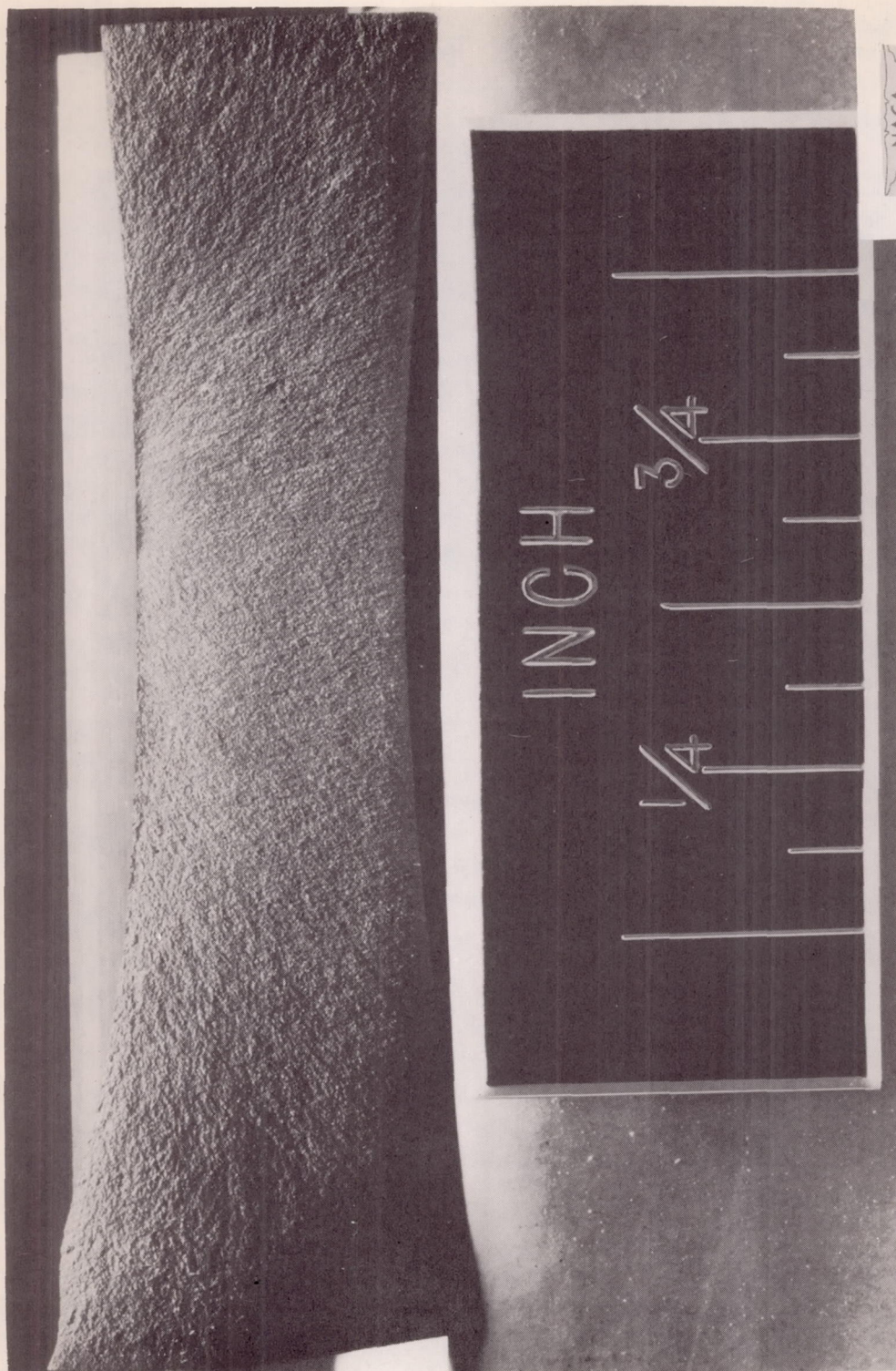


Figure 1. - Fracture surface of root failure in run 11.

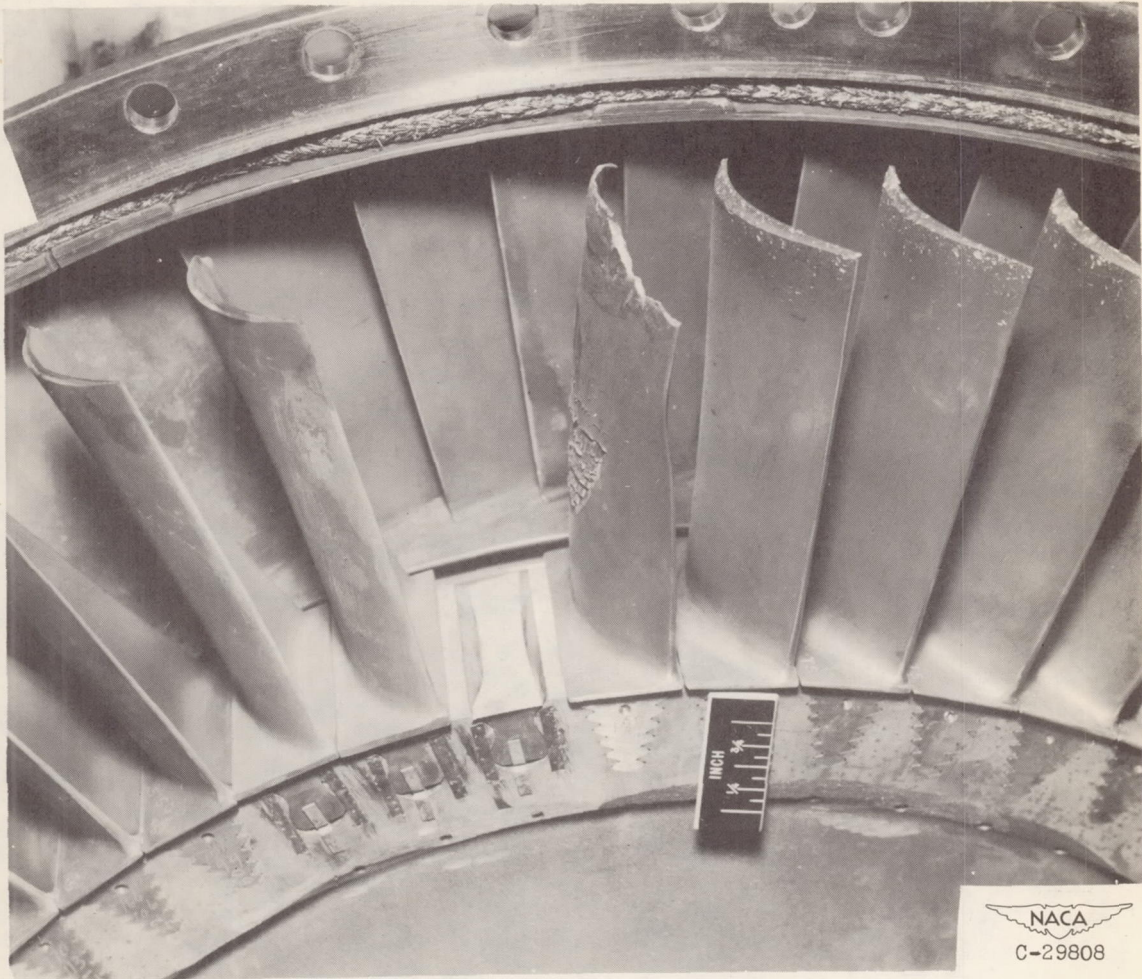


Figure 2. - Root failure in run 11.

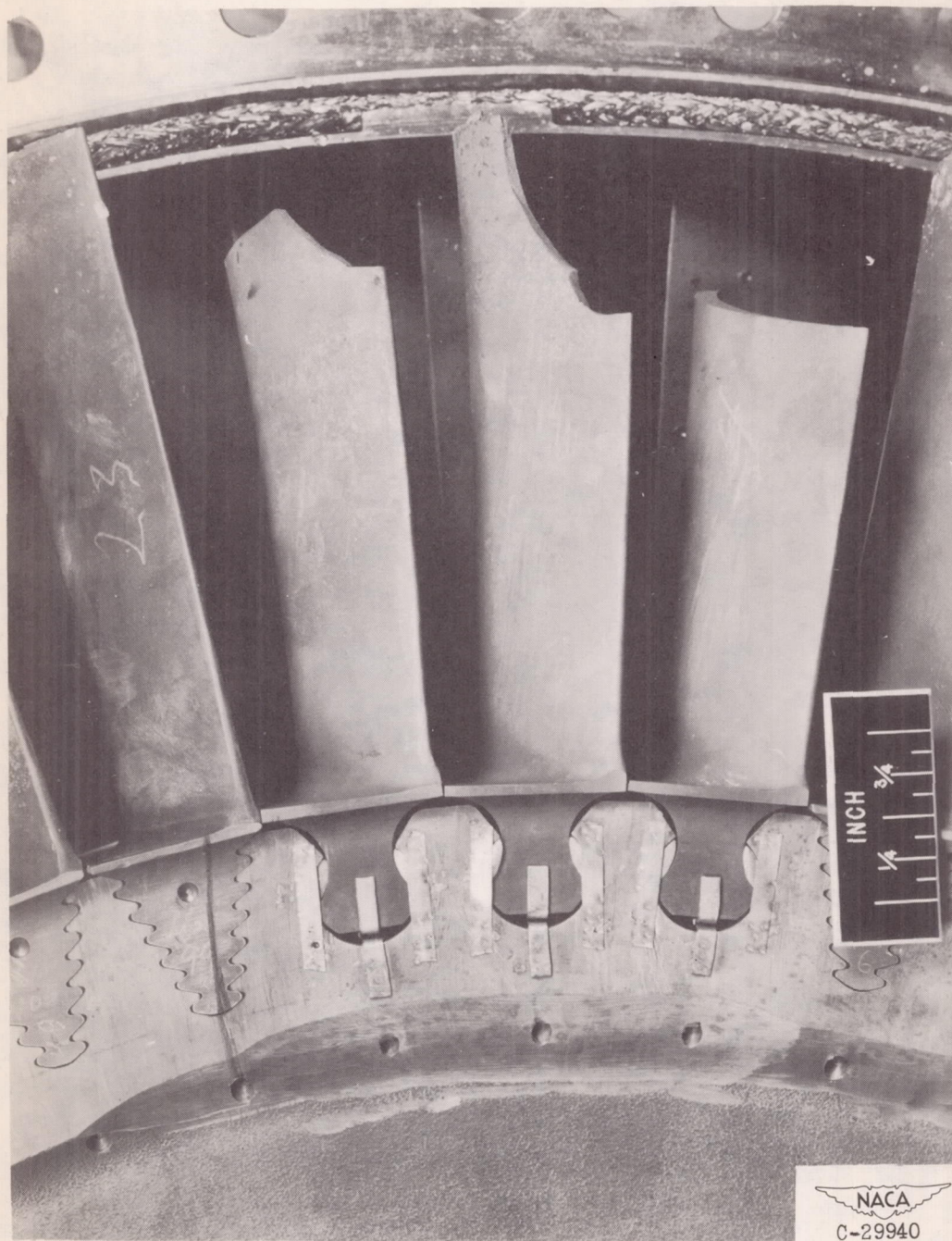


Figure 3. - Airfoil failures in run 11A.

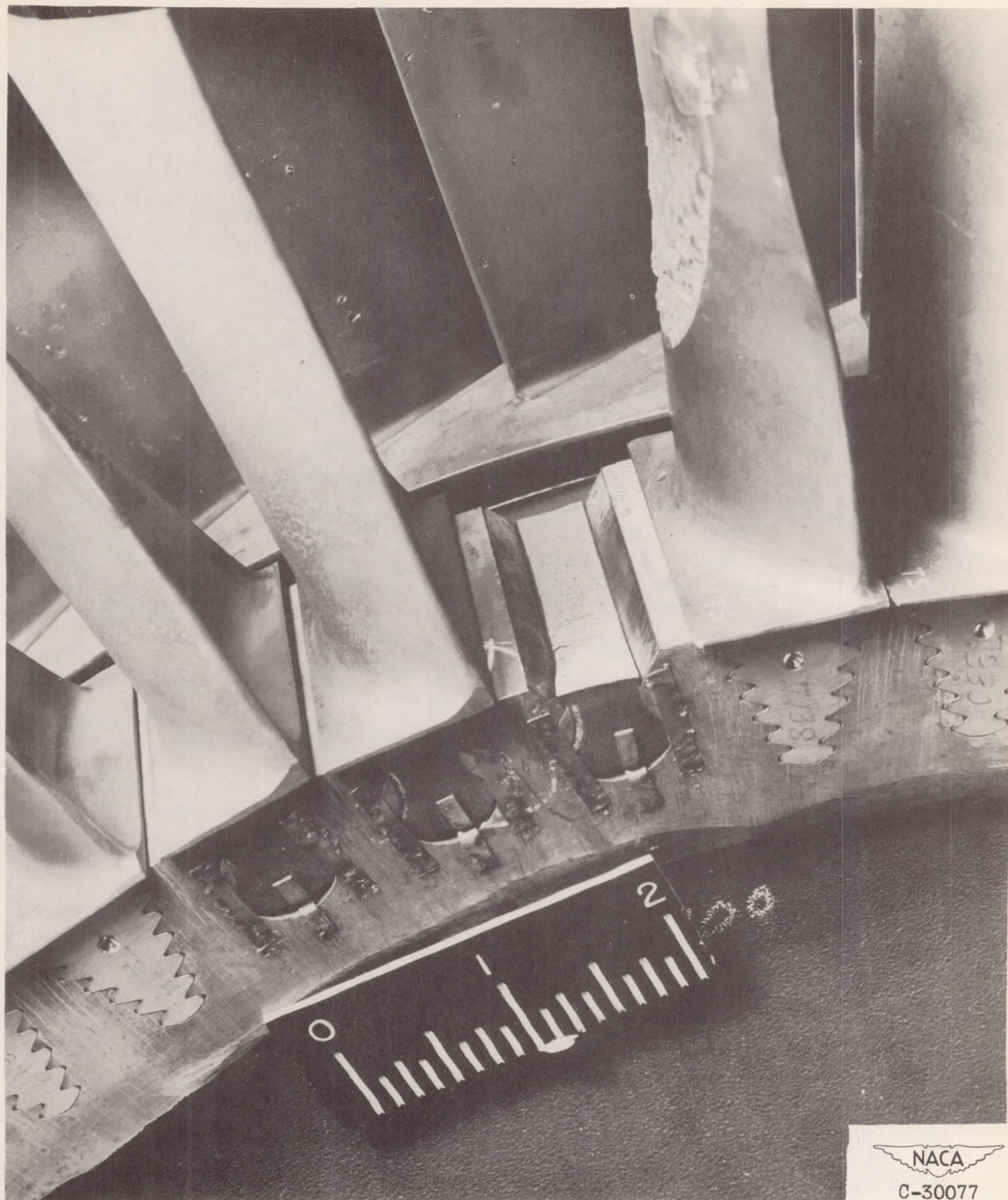


Figure 4. - Failure of blade with increased nickel content in root; run 12.



Figure 5. - Root failures in run 12A.

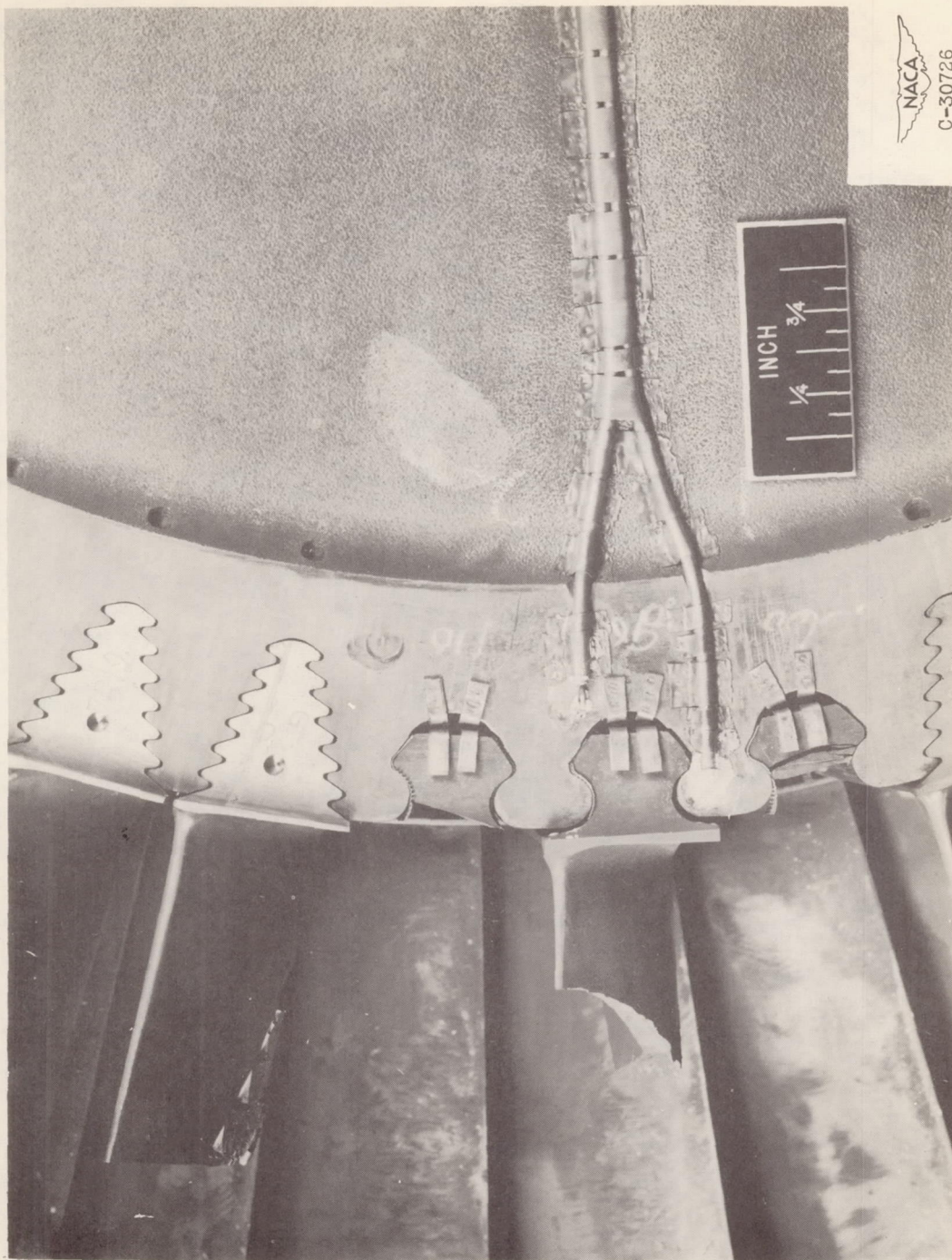


Figure 6. - Dovetail root failures of run 13.

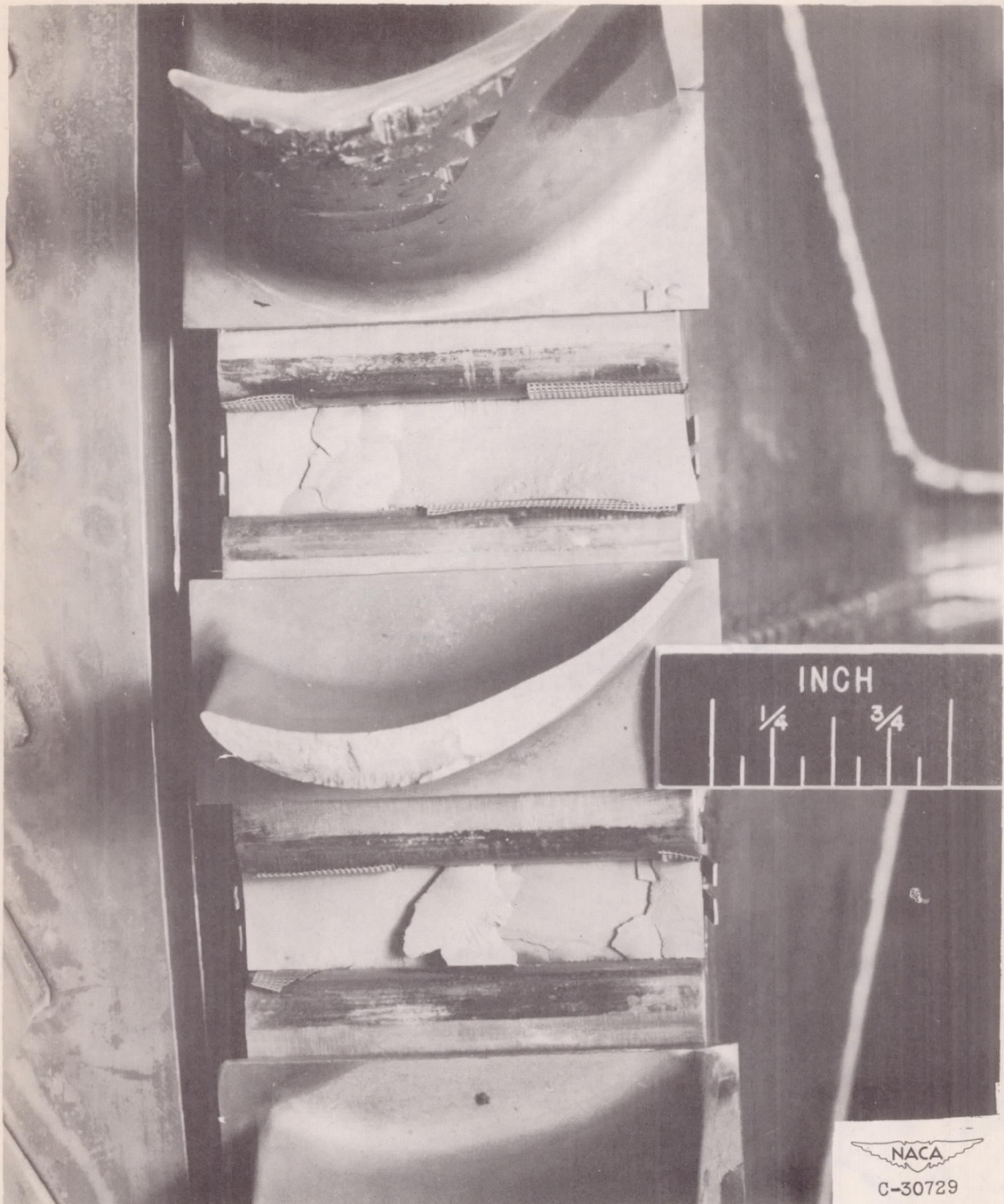


Figure 7. - Fracture surfaces of dovetail roots; run 15.

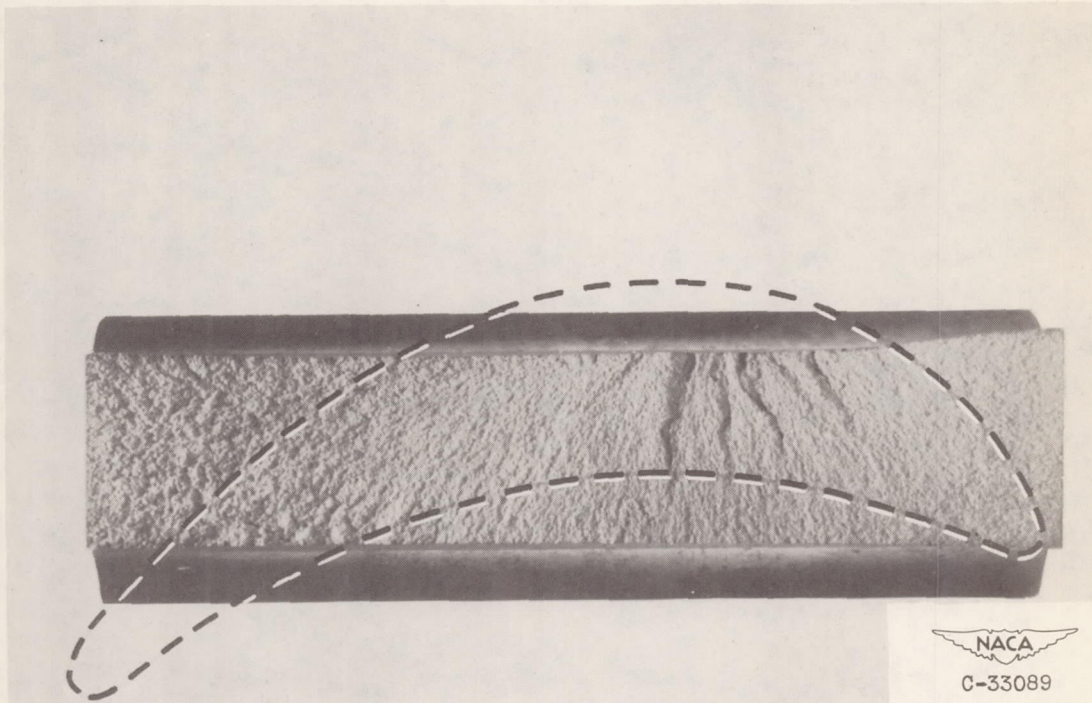


Figure 8. - Airfoil profile superimposed on failure surface.



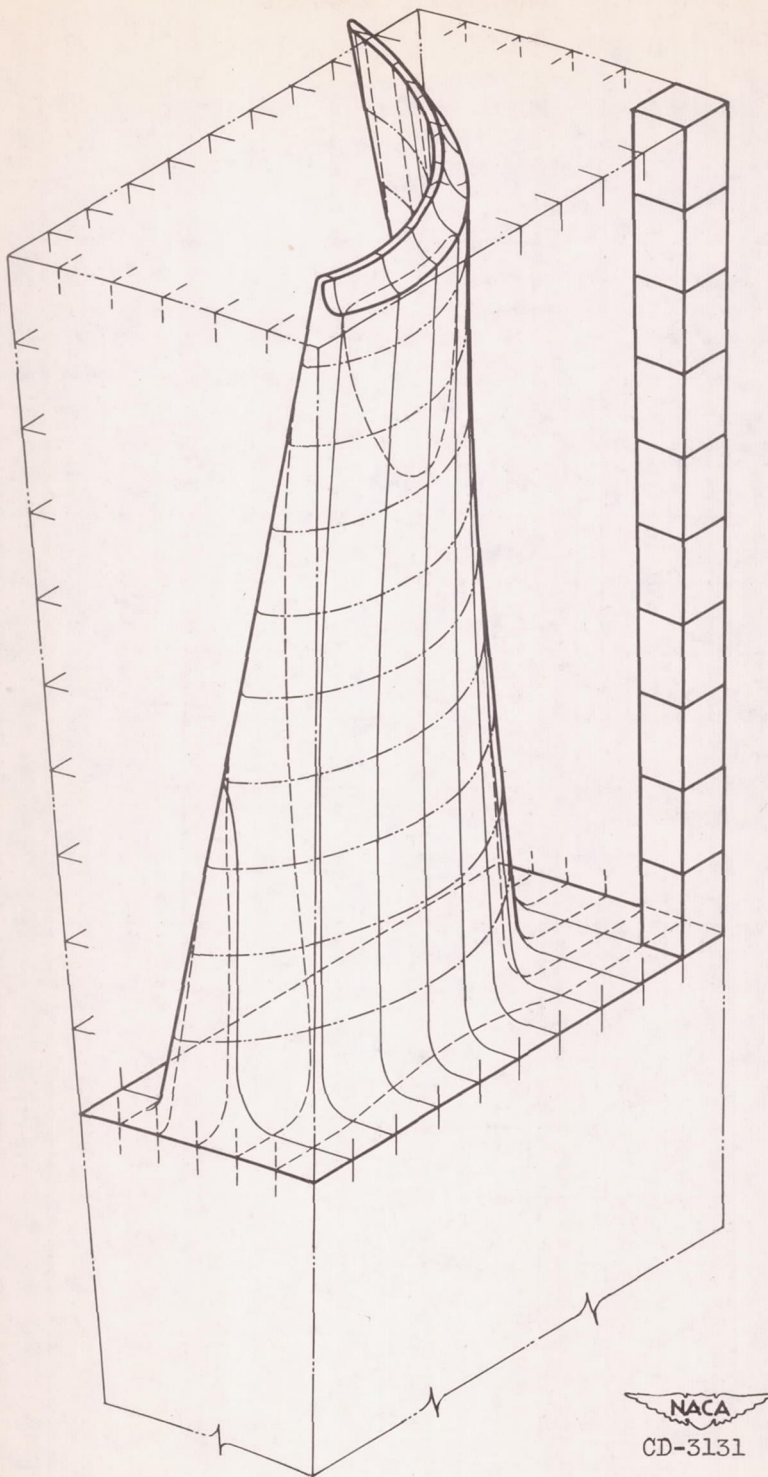


Figure 9. - Sketch showing airfoil divisions for computation.

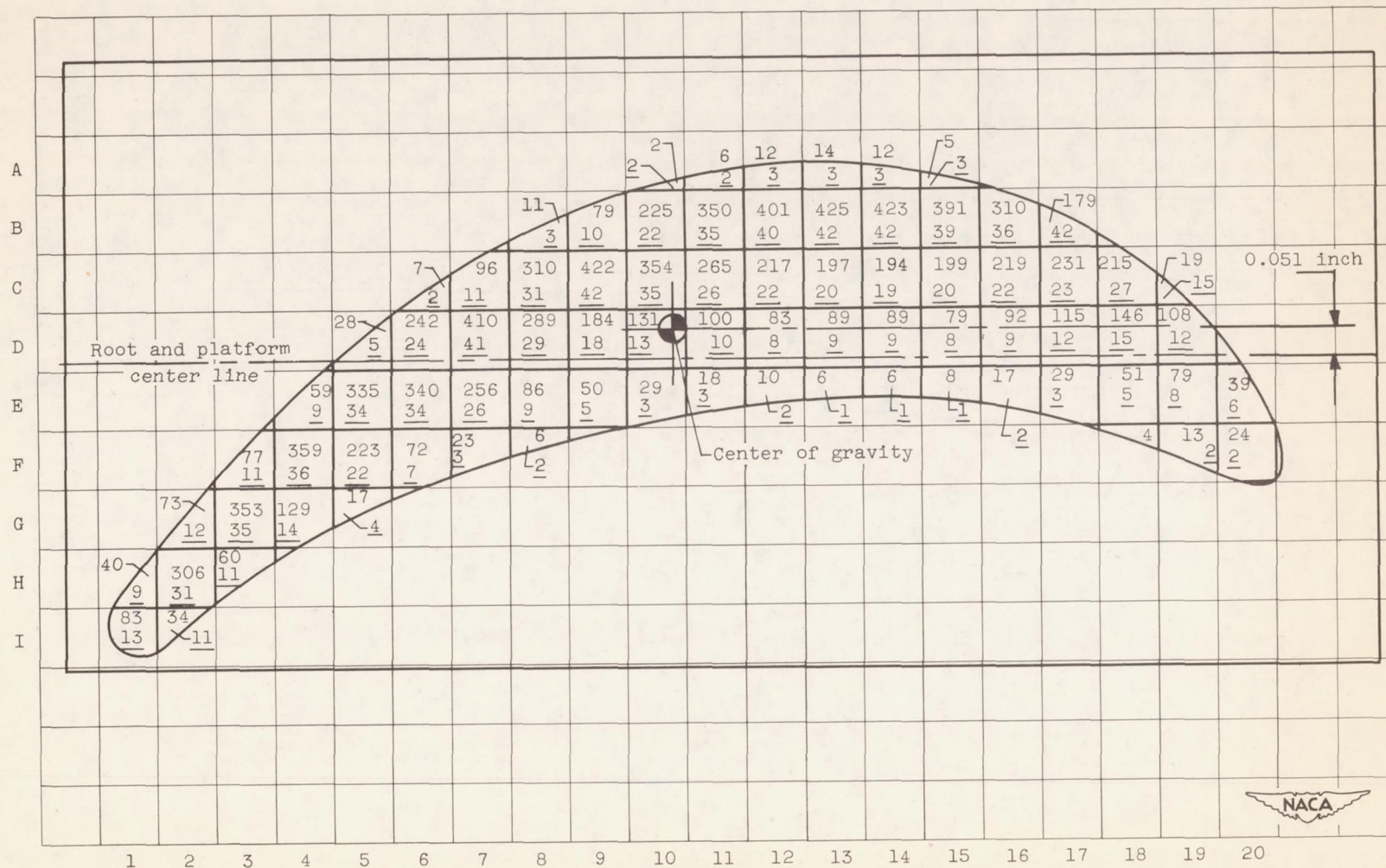


Figure 10. - Centrifugal force and stress distribution at base cross-section of airfoil.

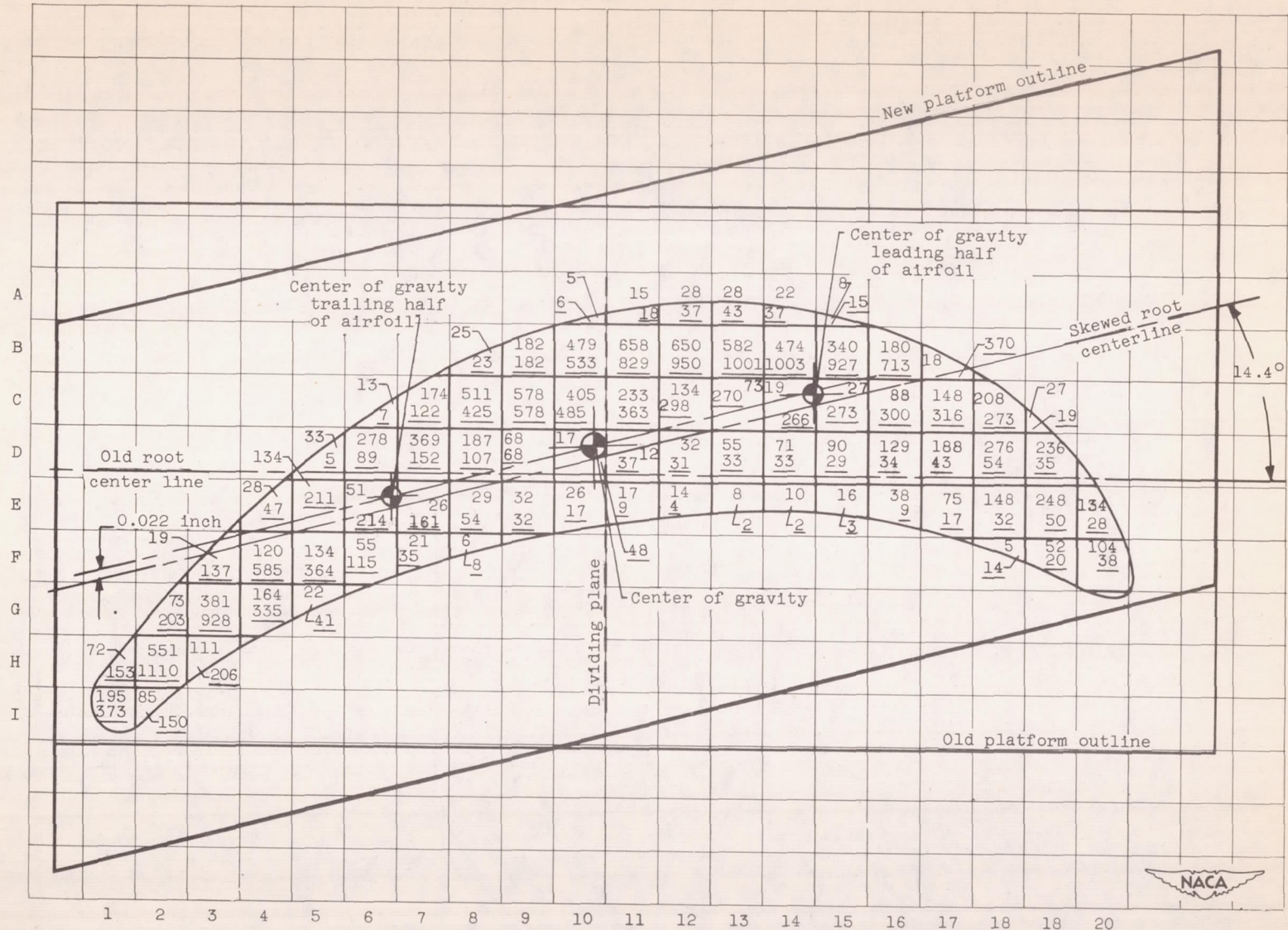


Figure 11. - Relative bending moment comparison for standard and skewed roots.

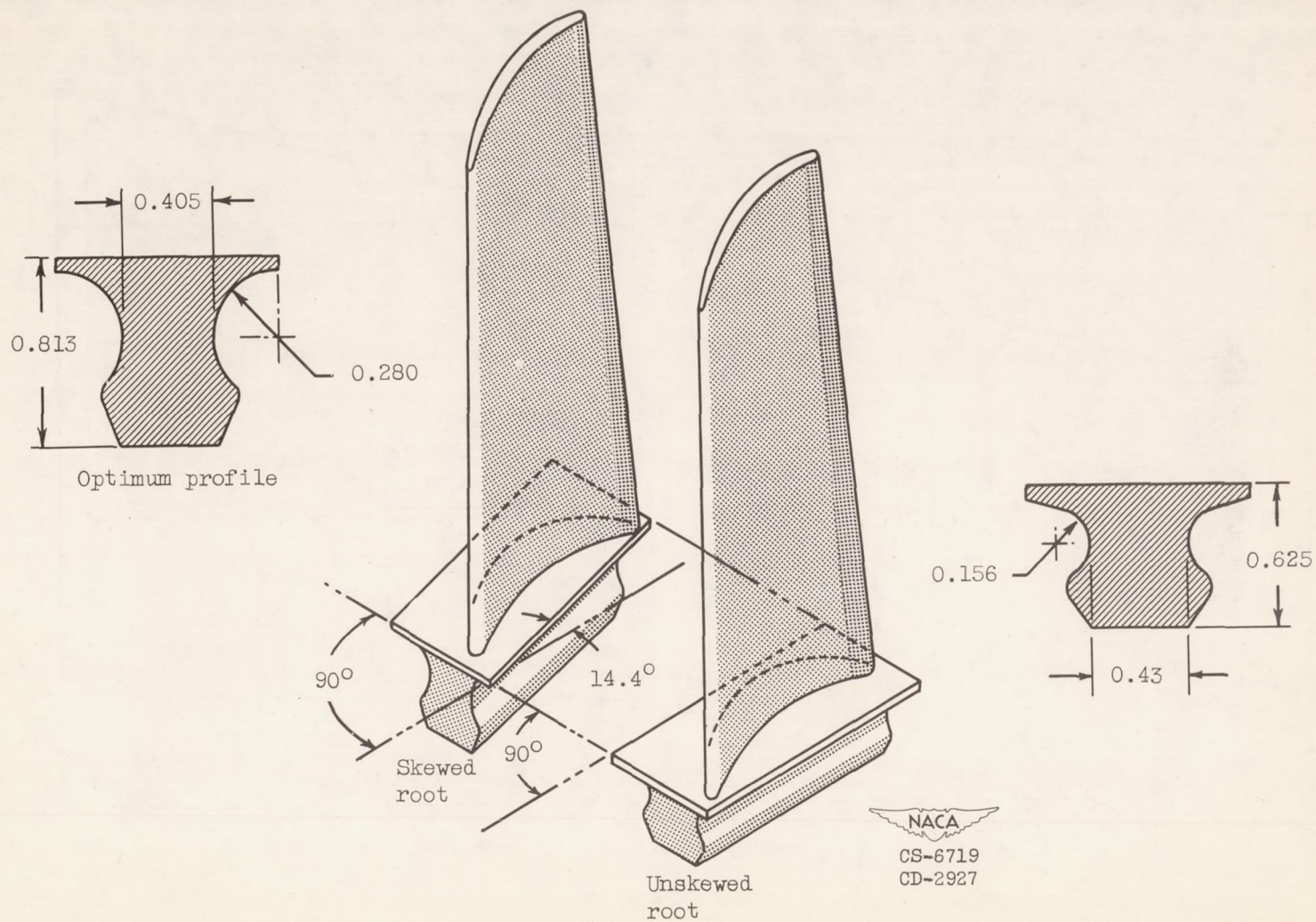


Figure 12. - Dimensions of standard and skewed dovetail cermet blades. (All dimensions are in inches.)

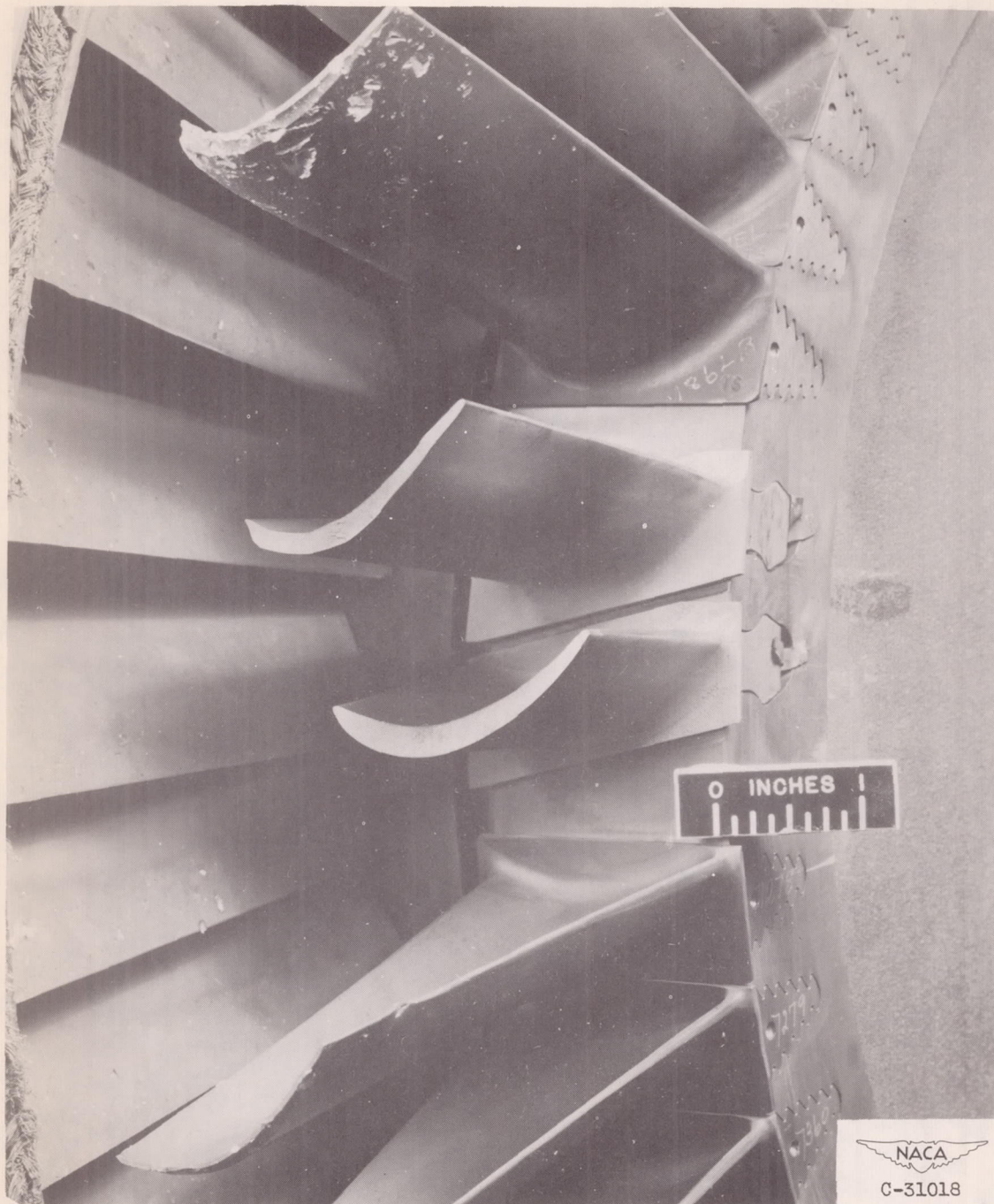


Figure 13. - Airfoil failures after 129.5 hours at rated speed; run 16.

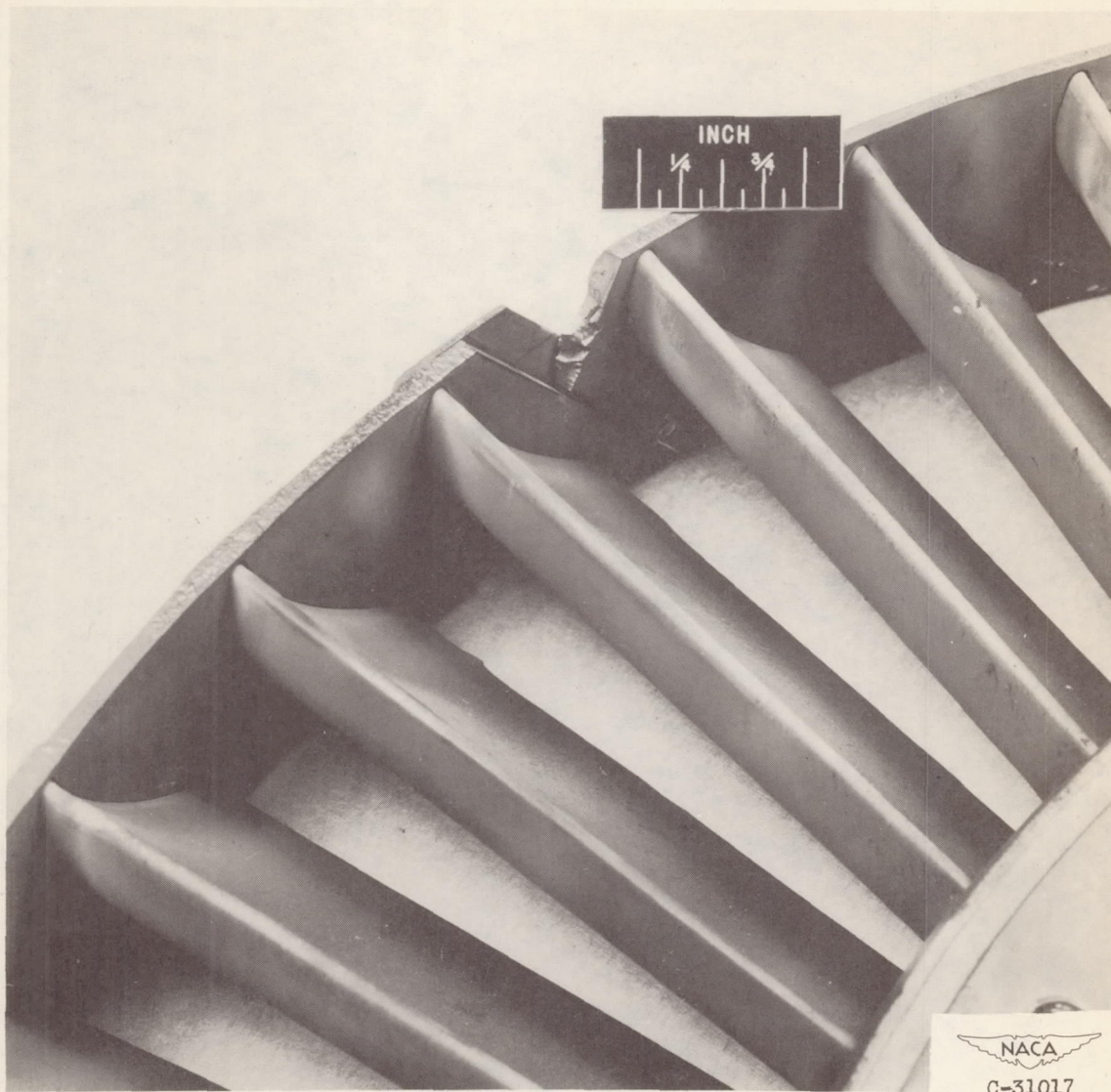


Figure 14. - Nozzle diaphragm failure which caused airfoil failures; run 14.

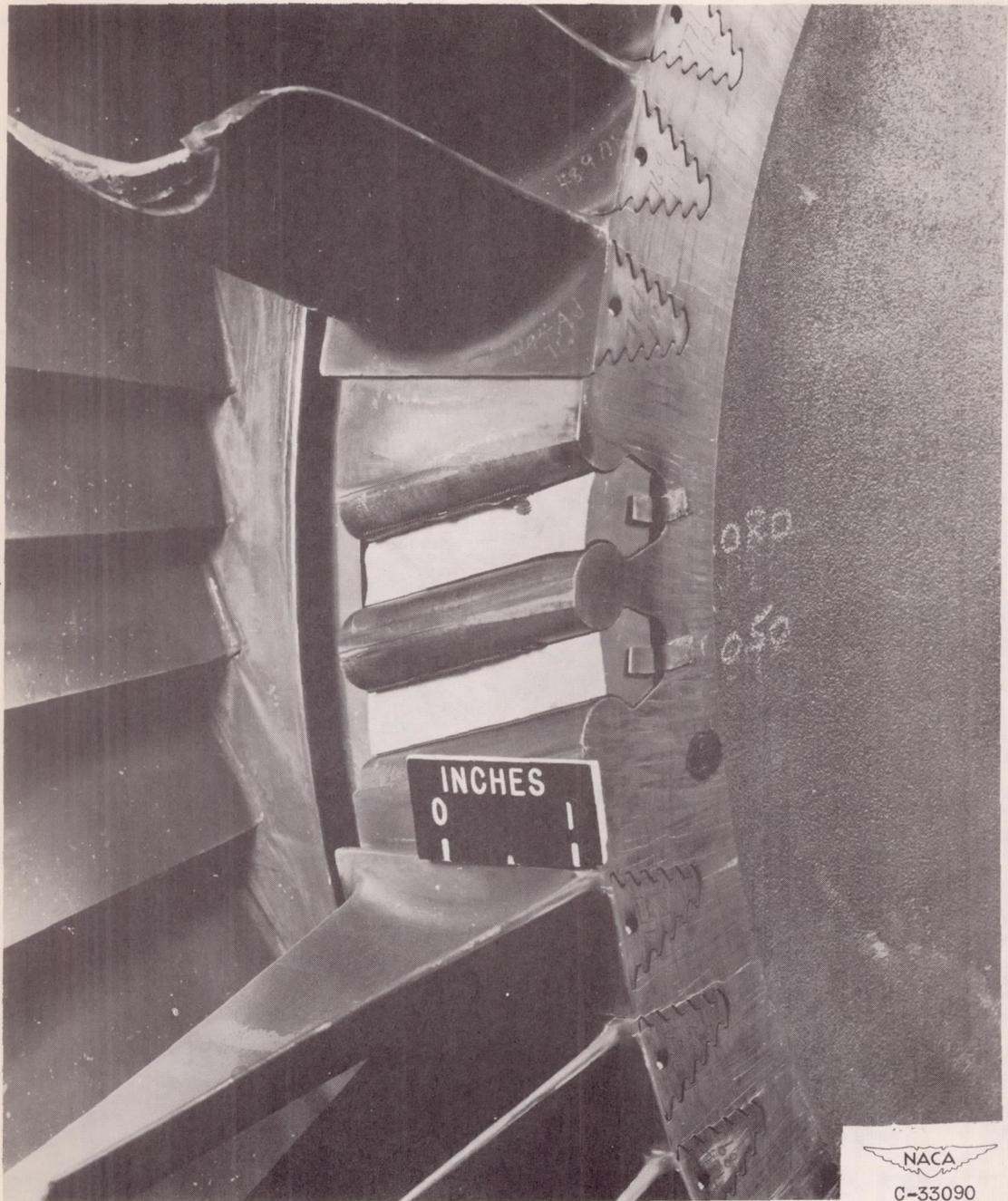
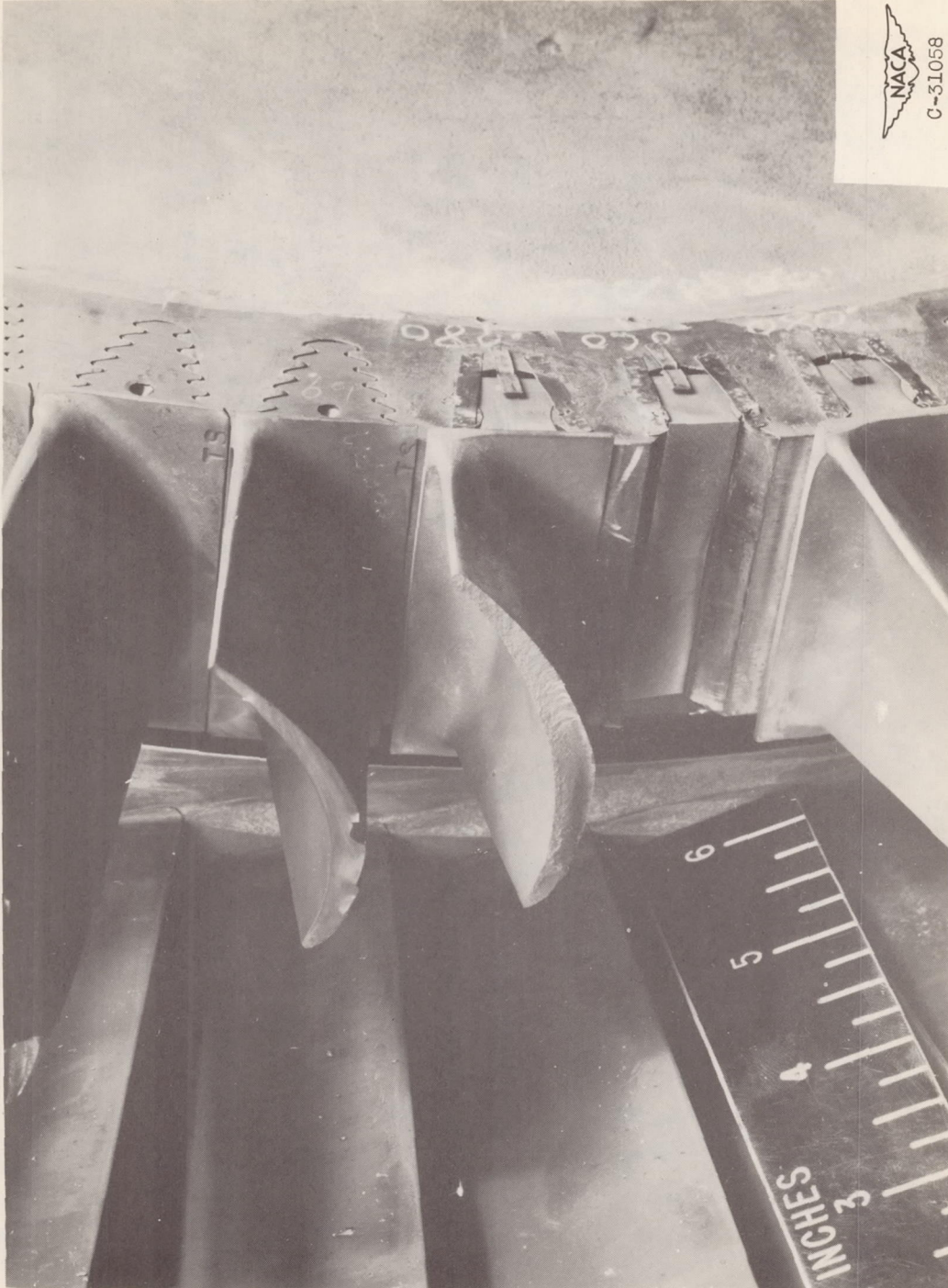


Figure 15. - Root failures after cyclic operation; run 15.



NACA  
C-31058

Figure 16. - Failure of interlock root made from refined material; run 16.



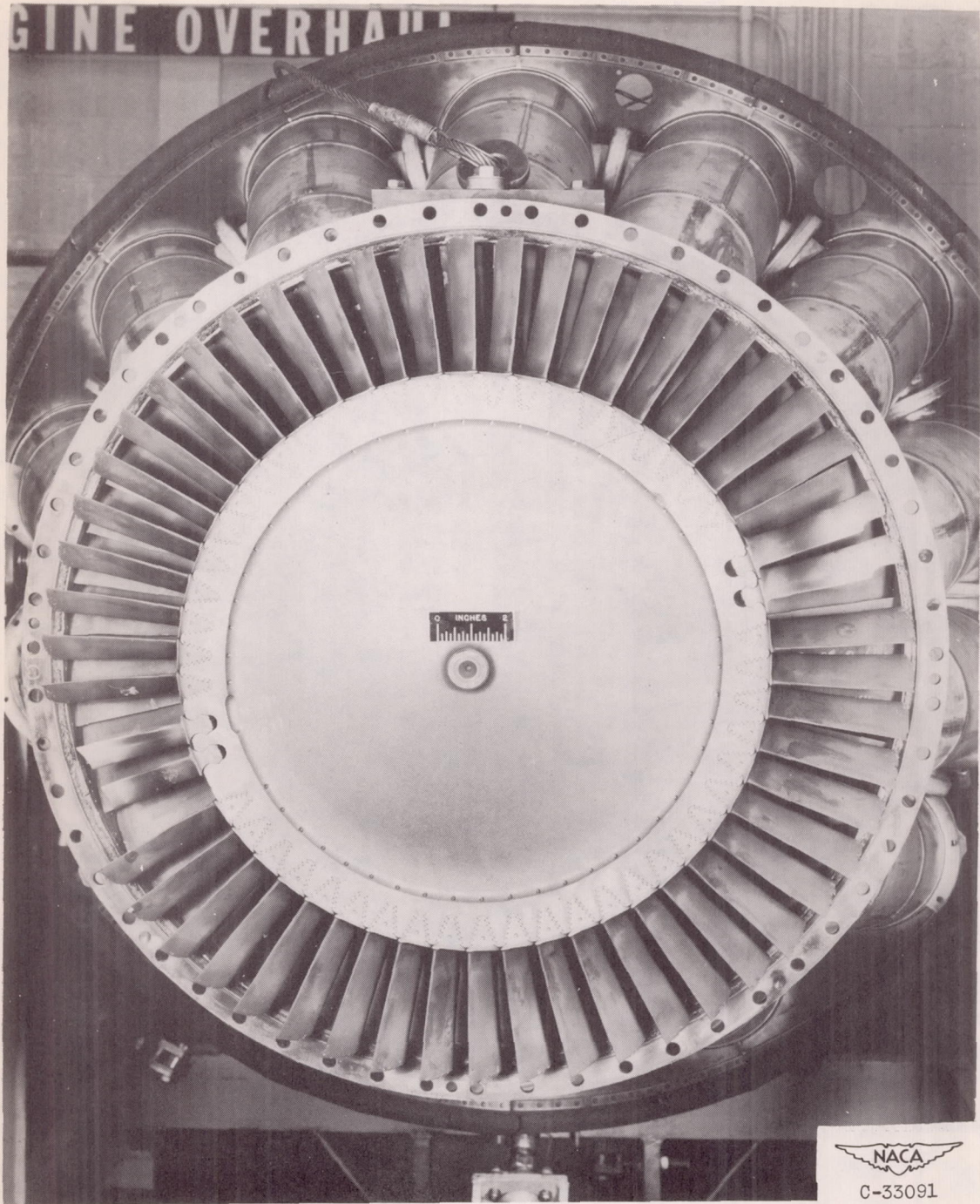


Figure 17. - Failure of airfoils resulting from fatigue of combustion domes and liners; run 17.

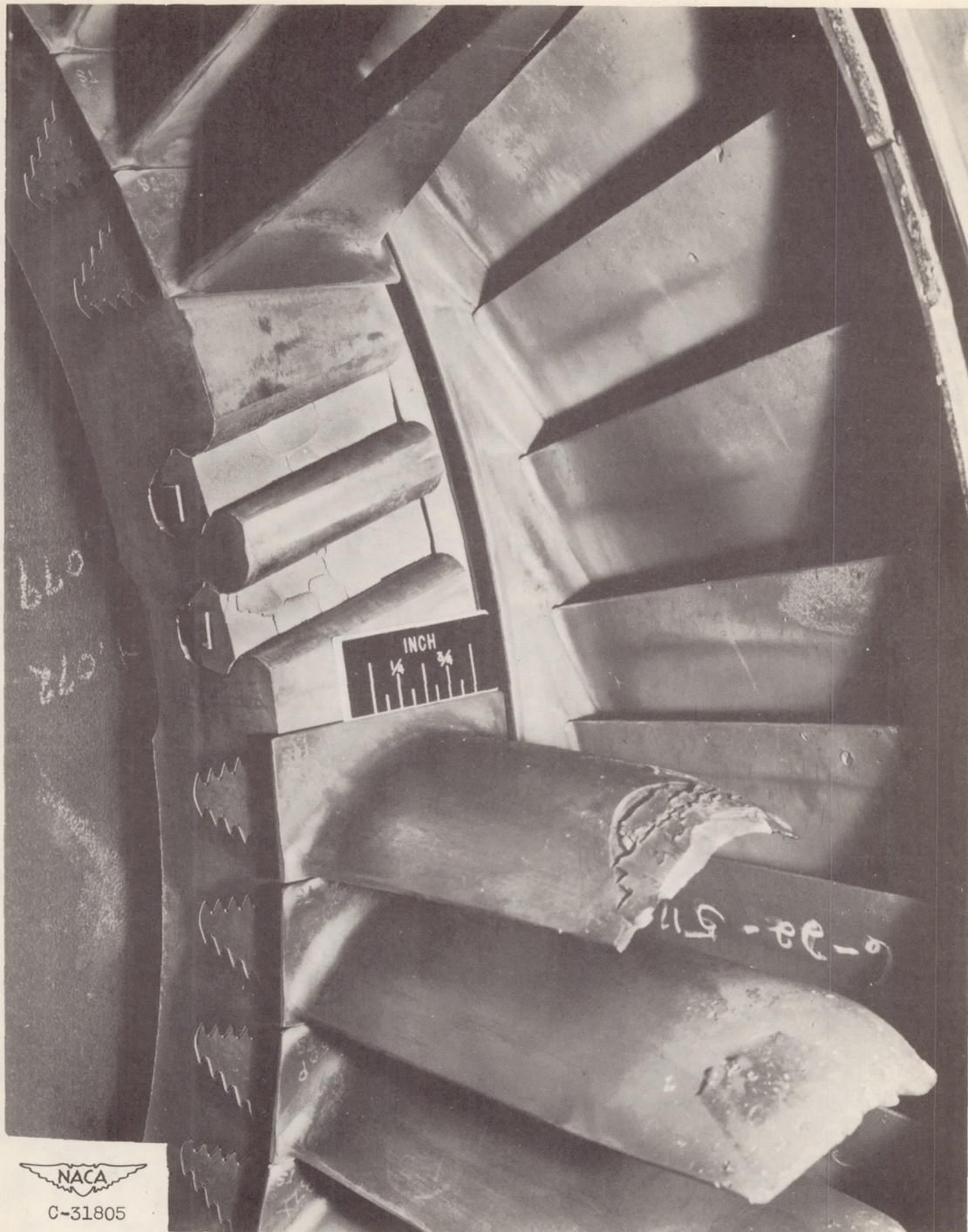
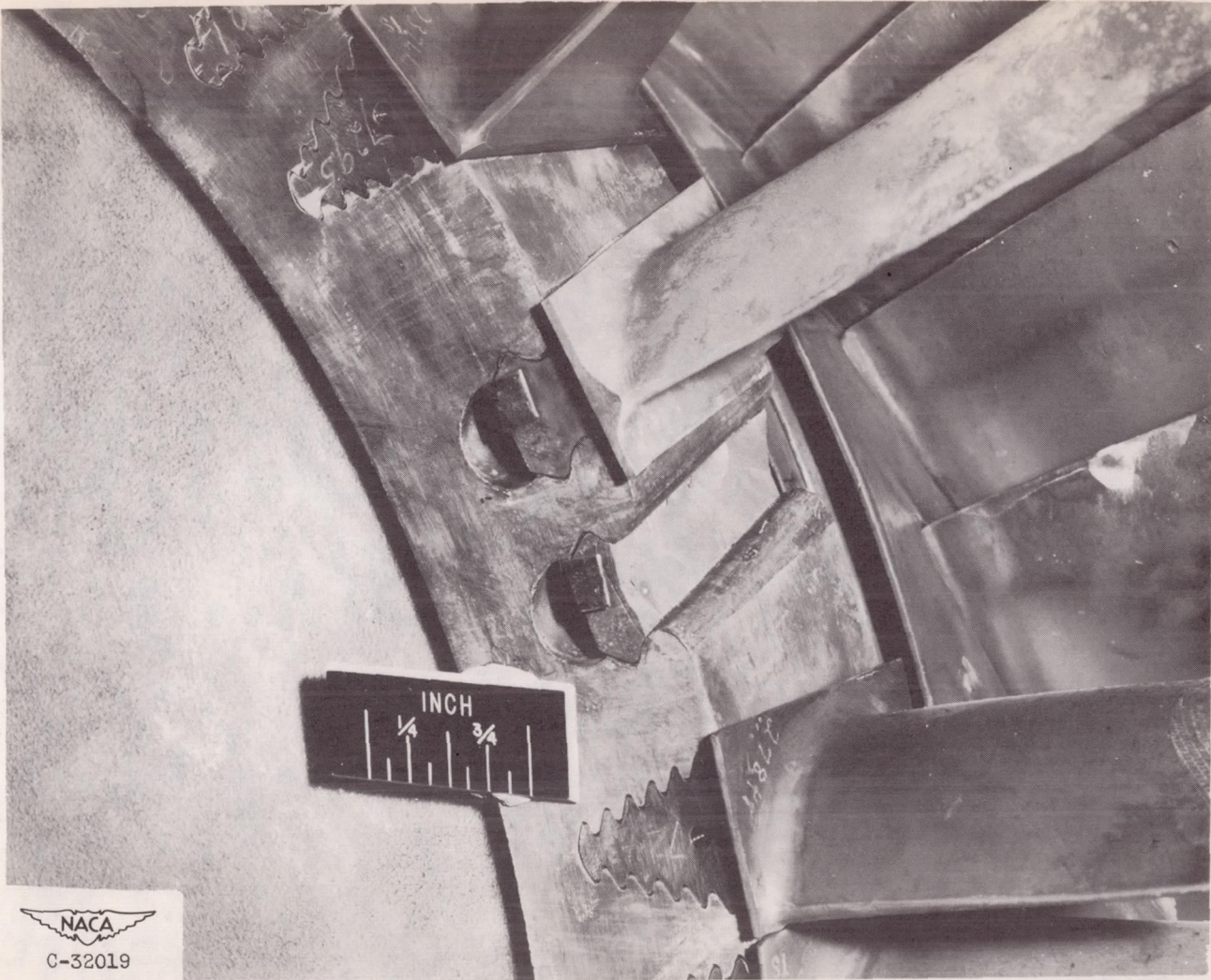


Figure 18. - Failure of skewed blades with large radii; run 18.



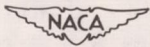
  
C-32019

Figure 19. - Failed roots of skewed blades with small radii; run 19.

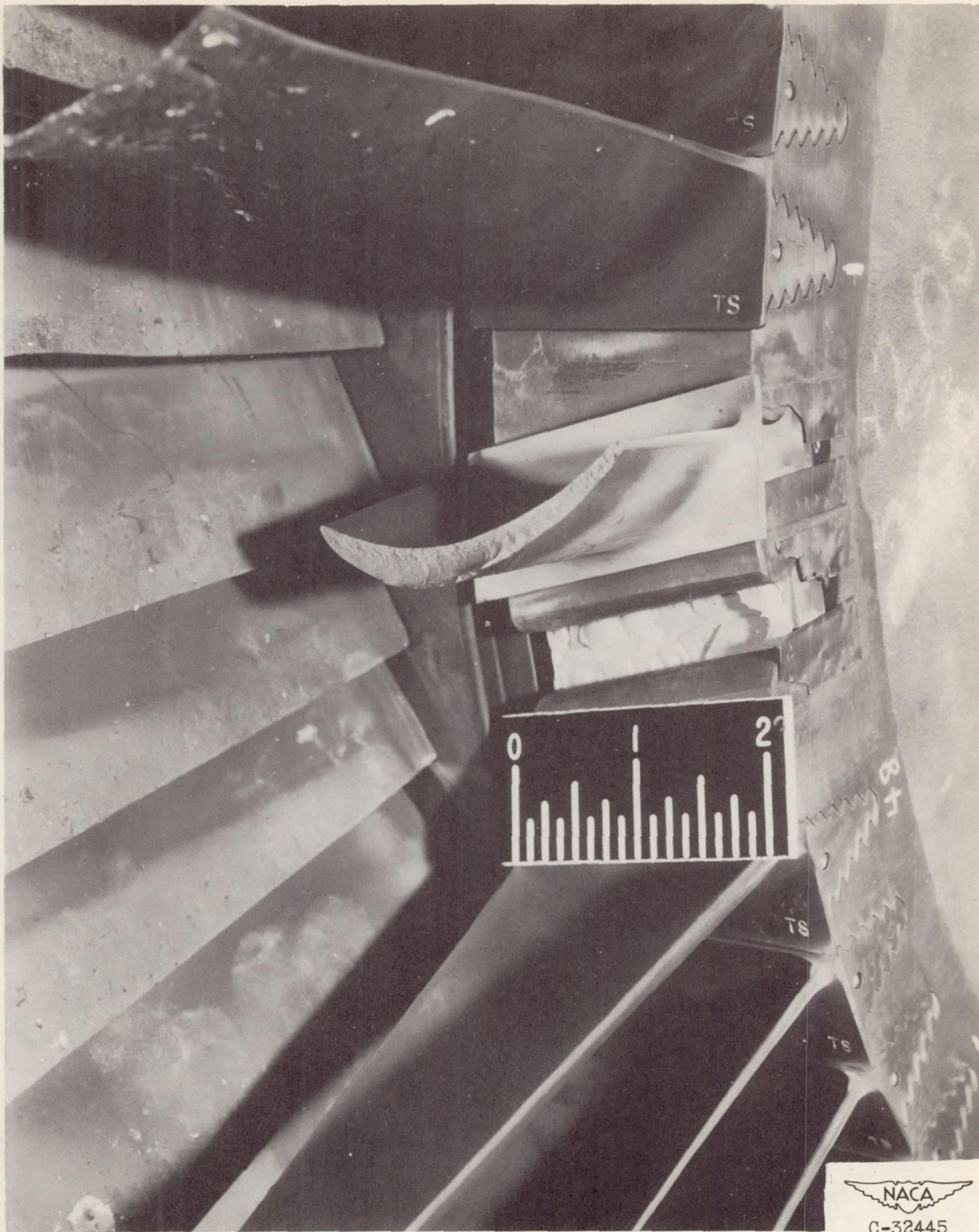


Figure 20. - Large-radius root failure after 108 cycles of 15 minutes at rated speed and 5 minutes at idle; run 20.